Surface characterization of the cuticle of *Dirofilaria immitis*

Fertac H. Bilge, Kamuran A. Kadipasaoglu, C. Michael McCormick, and Robert E. Baier

Department of Bioengineering, Clemson University, Clemson, South Carolina, and Department of Stomatology, and Interdisciplinary Sciences, State University of New York at Buffalo

The surface reactivity of the dog heartworm (*D. immitis*) was evaluated by comprehensive contact angle measurements and a platelet retention test. Contact angle data yielded calculated surface energy terms very similar to those previously reported for intact vascular endothelium. The platelet test revealed the native worm surface to be nonreactive, retaining fewer platelets than glass or worms whose surfaces had been modified by extraction with acid and high salt solutions. The cuticular morphology of the heartworm was studied with both light and electron microscopy, the latter coupled with ferritin-conjugated double-layer immunolabeling to reveal adsorbed host protein on the cuticle surfaces. Multiple attenuated internal reflection (MAIR) IR spectroscopy confirmed the general composition of this surface layer to be glycoproteinaceous. Morphological and histochemical studies confirmed and extended previous descriptions of nematode cuticle, adding ultrastructural detail on cortical, medial, and basal layers. A trilaminar membrane, apparently corresponding to a mammalian cell membrane (plasmalemma), constituted the external cortical layer as observed in high magnifications. The existence of a glycocalyx of varying thickness was demonstrated in ruthenium red-stained sections. MAIR IR spectra showed this glycoproteinaceous film to appear, in fully hydrated samples, as a loose biological gel. Ferritin–antibody conjugate labeling confirmed the presence of adsorbed dog albumin, dog immunoglobulin class G (IgG) and dog complement fraction 3 (C3) in the cuticular surface layer. It is likely, therefore, that *D. immitis* heartworms demonstrate long-term thromboresistance at least in part due to their passive low-surface-energy overcoating with host proteins.

INTRODUCTION

Incompatibility of blood with many foreign surfaces remains a major obstacle to the successful development of a greater variety of cardiovascular implants. In spite of impressive accomplishments made in recent years, scientific understanding of blood–foreign surface interactions, and development of new reliable, versatile blood compatible materials, still requires effort.[1]

Blood parasites have evolved in the bloodstream and perforce display thromboresistant surfaces. Among the numerous blood flukes, the dog

This work was supported by National Science Foundation Grant ECE-8504517, and the New York State Science and Technology Foundation.

Journal of Biomedical Materials Research, Vol. 23, 1027–1047 (1989)
© 1989 John Wiley & Sons, Inc. CCC 0021-9304/89/091027-21$04.00

heart worm, *Dirofilaria immitis*, is especially interesting because of its nail-like covering called the cuticle. *D. immitis* is a nematode that usually lives in the pulmonary artery and right heart of the dog. It is generally accepted that *D. immitis* is not responsible for the destruction of blood and its surface is always observed to be clot-free.

How does *D. immitis* achieve this hemocompatibility? One suggested mechanism is the spontaneous coating from blood of the cuticle with a benign layer of host proteins, such that this coat masks the parasite and it is not recognized as foreign.[2] For this and other suggested mechanisms for nonpathogenesis, the composition of the blood contacting surface, i.e., the cuticle, plays a critical role. Therefore, characterization of the cuticle of *D. immitis* was undertaken to improve our understanding of such important host–parasite relationships and provide some insight to mechanisms by which this blood-dwelling nematode achieves its hemocompatibility.

The chemical composition of the cuticle of nematodes is described in detail by Bird.[3] In general, the nematode cuticle consists of mostly water and protein with small amounts of lipid and carbohydrate. Various morphological studies have revealed the cuticle to be an acellular structure mainly composed of collagen- and keratin-like proteins. The outermost layers of the nematodes have been shown to include a glycocalyx, a carbohydrate-rich coat usually associated with single cell surfaces. This coat can include proteins, glycoproteins, and glycolipids that are incorporated within the plasma membrane along with adsorbed molecules, but the polysaccharide-rich quality of the surface coat in question here has been demonstrated (on the cuticle of *D. immitis* microfilariae) using cytochemical stains.[4] Lectin binding studies have shown that various extracuticular carbohydrate residues like D-mannose, D-glucose, N-acetyl-D-galactosamine and sialic acids are involved in nematode–host plant[5] and nematode–fungal predator[6,7] recognition as well as in chemo-attraction to food and mate.[8] The contributions of glycoproteins and of the carbohydrate moieties themselves to surface immunogenicity and hemocompatibility have recently been documented in the case of the human blood fluke *Schistosoma mansoni*.[9,10]

The proteins of the surface coats of parasitic nematodes have been studied by gel electrophoresis.[11] Host serum albumin was reported to be the major surface protein on the microfilaria of *L. carinii*. The presence of host proteins on the surfaces of adult and microfilarial stages of *D. immitis* have also been shown with fluorescent antibodies.[12] These findings support the hypothesis of molecular mimicry of the host. On the other hand, a heparin-like polysaccharide from the integument of *S. mansoni*[13] and a polysulfated polysaccharide on the surface of the cestode *Taenia taeniaeformis*[14] were shown to have anticoagulant activities.

Even though these latter observations suggest the use of an anticoagulant by some parasites to remain clot-free, the general significance of the physical–chemical surface properties for the survival of these flukes remains. This is especially true for the case of *D. immitis*, which possesses only an in-

active cuticle from which no active secretion has been reported. Hence, continued study of the surface of *D. immitis* may give us a better understanding of blood–foreign surface interactions by more complete characterization of this successful, intrinsically thromboresistant material.

In this report, the surface reactivity of the nematode is evaluated by comprehensive contact angle measurements and a platelet retention test. The cuticle is structurally characterized using light and transmission electron microscopy. The presence and general composition of the exterior layers is shown using IR spectroscopy and electron microscopy, and the presence of host proteins within this layer is demonstrated by antibody labeling results.

MATERIALS AND METHODS

Female *D. immitis* worms were obtained as a gift from Dr. J. McCall, Department of Parasitology, University of Georgia, Athens, GA. Originally frozen worms were used for hemocompatibility analyses based on platelet retention criteria, for light microscopy to study the structure of the cuticle and, together with never-frozen worms, for electron microscopic studies of their surface coats.

Hemocompatibility

The surfaces of *D. immitis* were evaluated using a customized platelet retention test.[15] Briefly, citrated whole canine blood was passed over the worms in a test chamber, and platelet adhesion to the surfaces was evaluated by platelet counts of the blood before and after contact with the worms. Platelet adhesion to the cuticular surfaces was confirmed by scanning electron microscope visualization of the surfaces. Additional tests were performed on *D. immitis* that had been exposed to high electrolyte concentration (0.75*M* buffered saline) and low pH (acetic acid buffer pH = 4) solutions for 35–40 min in attempts to alter the surface coatings. Following such exposures, the worms were removed and viewed by SEM and the supernate was analyzed for protein content using Folin-Cochitine analysis.

Light microscopy

The frozen *D. immitis* worms were thawed, sectioned, and fixed in 10% buffered neutral formalin. The histochemical method of Ayoub-Shklar was used for keratin and collagen analysis. Routine Mayer's H&E staining was employed to enhance cellular detail. A dog foot pad was used as control material for the analytical and morphological studies in each case.

Electron microscopy (TEM)

Fresh female worms, obtained from the same laboratory, were transported in culture medium RPMI-1640 (Gibco Ltd., Grand Island, NY). Some were frozen upon arrival at Clemson and kept frozen at −20°C until used. Worms were thawed on the day of the experiment and rinsed in 0.1*M* cacodylate rinsing buffer (CRB), pH 7.4 (21.4 g/L sodium cacodylate and 73 g/L sucrose). The worms to be used in ferritin-labeling experiments were incubated in a 1% solution of Bovine Serum Albumin (Miles Scientific, Naperville, IL) in cacodylate fixing buffer (CFB, 21.4 g/L sodium cacodylate), pH 7.4, for 30 min, to cover the nonspecific binding sites on the cuticle surfaces. The worms were then directly transferred to test tubes containing the primary antisera, where they incubated for 30 min at room temperature.

Rabbit anti-dog whole serum (RAD-WS, Miles), rabbit anti-dog albumin (RAD-A, Cappel Worthington, Cooper Biochemical, Talvern, PA), rabbit anti-dog complement fraction C3 (RAD-C3, Miles), and rabbit anti-dog immunoglobulin G (RAD-IgG, Miles) were used in different tubes as primary antibodies. Following a rinse in CRB three times for a total of 30 min, the worms were allowed to incubate in horse spleen ferritin conjugated to anti-rabbit IgG produced in goat (F-GAR-IgG, ICN Immunobiologicals, Lisle, IL) for 30 min. All immunoglobulins were diluted 1:40 in CFB. After a final rinse in CRB twice for 15 min each, the worms were sectioned in three pieces of equal length; the head and tail portions were discarded and the middle piece was further sectioned in pieces of approximately 5 mm each.

Sections were fixed in 4% glutaraldehyde in CFB for 2 h followed by 2% osmium tetroxide in CFB for 1 h, dehydrated in an ethanol series and infiltrated with propylene oxide twice for a total of 30 min. Worms selected to yield morphological sections were rinsed in CRB and sectioned as described above and then transferred into a mixture of 4% glutaraldehyde and 0.8% ruthenium red in CFB, pH 7.4 for 2 h, followed by a mixture of 2% osmium tetroxide and 0.8% ruthenium red in CFB, pH 7.4 for 2 h. Dehydration and infiltration were performed as described above, simultaneously for all test specimens.

Spurr's low viscosity embedding medium was used to achieve penetration through the hard cortical layer of the cuticle. The specimens were passed gradually from the infiltrating agent to the embedding medium, using ratios of 2:1, 1:1, and 1:2, each for 24 h. After a final soak of 24 h in pure embedding medium, each piece was cured under vacuum at 60°C for 48 h. Cured specimens were trimmed and sectioned on a Reichert-Jung ultramicrotome with a diamond knife (DuPont Instruments).

Thin sections, approximately 65 nm thick, were collected on acid-washed hexagonal copper grids (Electron Microscopy Sciences) and stained with uranyl acetate at 20°C for 12 min followed by lead citrate at 60°C for 45 min in a 2168 Ultrastainer Colsberg System (LKB Bromma). Stained sections were viewed with a JEM-100C electron microscope (JEOL LTD) at 60 kV.

Three additional groups of worms were processed as surface, primary antibody and secondary antibody level controls. The surface level controls

were prepared by stripping off any surface proteinaceous coat in an acetate–acetic acid solution (6.37 g/L sodium acetate, 1.5% glacial acetic acid, 3 g/L sodium chloride) of low pH and high ionic strength for 2 h. The primary antibody level controls were treated with nonimmune rabbit whole serum (Cappel) in place of the primary antibody in the above-described procedure. The secondary antibody level controls incorporated those worms which were treated in RAD-WS as primary antibodies, but were incubated in unconjugated 2× crystallized ferritin (Polysciences, Inc., Warrington, PA) instead of F-GAD-IgG, as well as worms for which the primary antibody layer was omitted.

Surface chemistry

Fresh specimens were placed in 0.15*M* PBS, pH 7.4, 2.5% glutaraldehyde solution until prepared for both comprehensive wettability profiling (via contact angle measurements) and surface spectroscopy (via multiple attenuated internal reflection infrared measurements).

The preparation technique consisted of distilled water rinsing of the individual filamentous worm bodies, and their mounting as suspended strands—without being put under tension—across the central region of a small, all-Teflon "embroidery hoop" device. Contact angle data were taken by direct droplet measurements along the lengths of these strands after they had air-dried. Infrared spectroscopy was performed by cutting short, straight segments of these filaments and pressing them tightly against miniature internal reflection prisms made from pure germanium, and mounting the assembly in a condensing mirror optical device within the sample compartment of a standard recording infrared spectrophotometer.

RESULTS

Hemocompatibility

The platelet count for each blood sample was done in duplicate. These values were used to calculate retention ratios to compare the properties of the different specimens tested. The average platelet counts and the platelet retention ratios for three different *D. immitis* surface states and for glass control specimens are presented in Table I. A simple *t*-test was used to determine if any significant differences existed between the retention ratios of native *D. immitis* and the other surfaces tested. The retention ratios for all the other substrata tested were significantly different from that for the native *D. immitis*.

Scanning electron microscopic (SEM) studies of *D. immitis* surfaces showed very little platelet adhesion (Fig. 1). The high salt and acid extracted specimens did not show any obvious alterations of the surfaces, but many additional platelets were seen to remain attached to their surfaces with moderate pseudopodial extensions. The glass surfaces had about the same number of

TABLE I
Retention Ratios

Material	Trial #	Control Count	Average Exposed Platelet Count	Retention Ratio
Native *D. immitus*	1	242,000/mm^3	236,000/mm^3	0.025
	2	297,000	274,000	0.077
	3	256,000	242,000	0.055
Acid extracted *D. immitus*	1	420,000	367,000	0.126
	2	483,000	408,000	0.155
	3	306,000	248,000	0.190
Glass	1	310,000	281,000	0.094
	2	417,000	300,000	0.281
	3	375,000	297,000	0.208
Salt extracted *D. immitus*	1	367,000	280,000	0.237
	2	264,000	157,000	0.405
	3	339,000	273,000	0.195

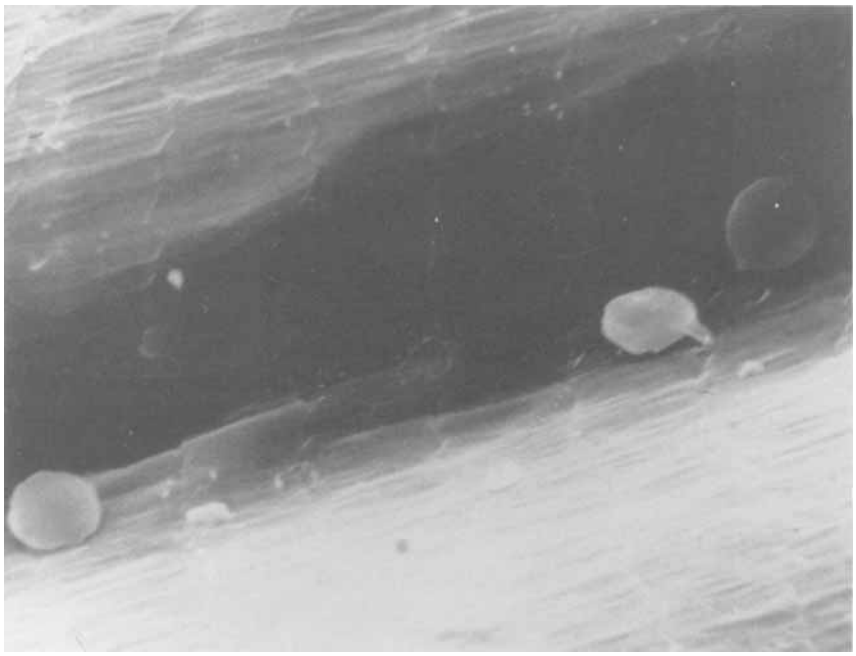


Figure 1. Surface of *D. immitis* following a platelet retention test (original magnification ×1300). Notice the lack of platelets even around the irregular areas of the body cavity.

retained platelets as the extracted *D. immitis* specimens. One observed distinction was the even greater degree of pseudopodial extensions from the platelets on glass.

Folin analyses confirmed the presence of extracted proteins in both the salt and acid supernates (7.8–55 mg/worm).

Light microscopy

All sections revealed a central body cavity (Fig. 2) containing the digestive tract and the reproductive organs, a surrounding muscle layer, nerve bundles and an outermost cuticle. In higher magnifications (Fig. 3), the cuticle was observed to consist of three distinct layers: the exterior cortical layer was essentially amorphous and stained with aniline blue specific for connective tissue, especially collagen. The median layer contained collagen-like fibers staining with aniline blue wrapped around a keratin-like material staining with orange G. The basal layer showed characteristic fine aniline blue-staining striations in most of the sections.

Electron microscopy

Examination of the tissue with TEM revealed the ultrastructure of the cuticle in greater detail. The observed general pattern of cuticular design was similar to that seen with the light microscope, but the cortical layer was further resolved into external and internal structures. The latter was similar to a cellular trilaminar membrane, approximately 15 nm thick (Figs. 4, 9) as described by Bird. The former consisted of a generally amorphous osmiopho-

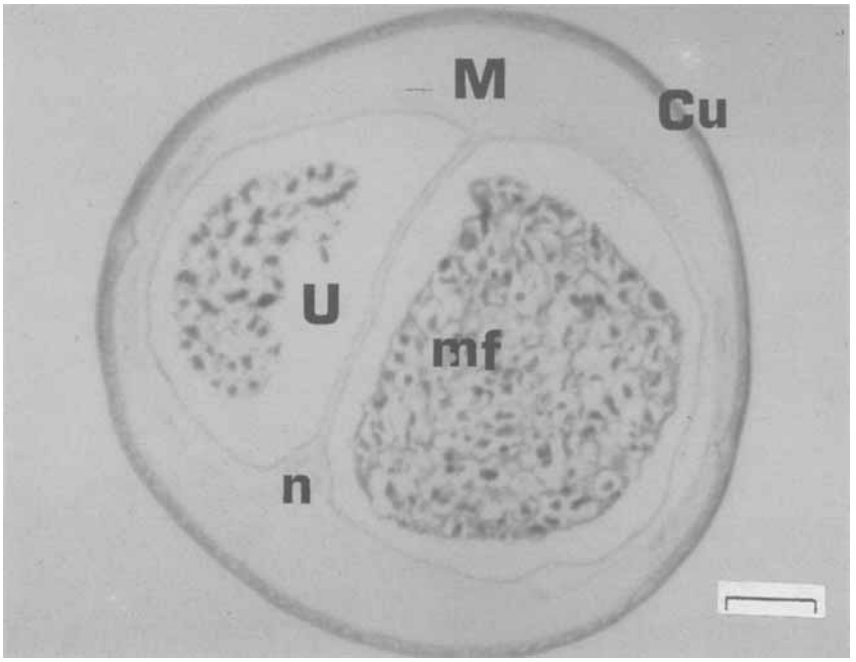


Figure 2. Light micrograph of *D. immitis*. Cross section of whole body (Hematoxylin-Eosin stain, ×60.) Bar = 200 μm. (b) basal layer, (Cu) cuticle, (c) cortical layer, (m) median layer, (h) hypodermis, (M) muscle, (n) nerve bundle, (mf) microfilariae, (U) uterus.

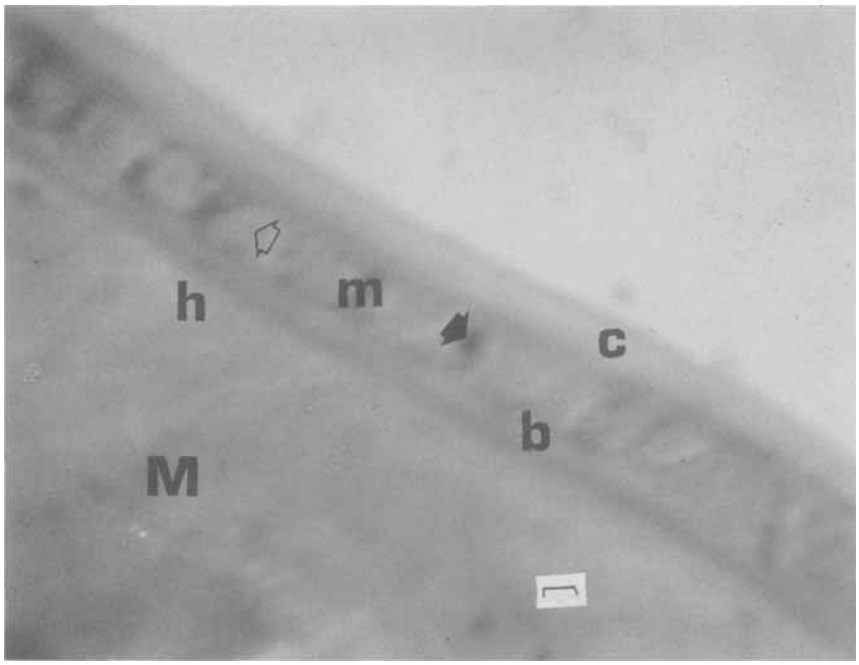


Figure 3. High magnification of Figure 2 showing cuticular layers. Note collagen-like fibers (closed arrow) wrapped around a keratin-like material (open arrow) (Orange G and Aniline blue stain, ×370). Bar = 10 μm.

bic layer approximately 5 μm thick (Fig. 4). The median layer was also observed to consist of external and internal structures, approximately 10 and 20 μm thick, respectively, separated from each other by an electron luscent band only 1 μm thick. In the external median layer, an electron dense band crossed an osmiophobic material at varying angles to the cuticular surface, but in some micrographs the entire bulk of the internal medial layer was osmiophobic. Characteristic striations of the basal layer (Fig. 4), were observed in most sections, and these connected internally with the hypodermis. A glycocalyx was clearly seen in sections stained with ruthenium red (Fig. 5) as a 10–50-nm-thick layer attached externally to the epicuticle. It was also visible in some immunolabeled tissue micrographs as a cloudy osmiophilic background beneath the ferritin layer (Figs. 6–8).

A continuous distribution of the ferritin particles was observed on immunolabeled surfaces for each of the four primary antibody types: anti-dog whole serum (RAD-WS), anti-dog albumin (RAD-A), anti-dog immunoglobulin G (RAD-IgG), and anti-dog complement fraction C3 (RAD-C3) (Figs. 6–9). RAD-A reacted the most vigorously with parasite surfaces (Fig. 7), while RAD-C3 was the least reactive (Fig. 9). At some locations, particles formed a multilayered coat. Control surfaces, on the other hand, showed no significant binding of ferritin (Figs. 10–12) with the exception of a few cases (Fig. 13) in which there was insufficient stripping of the proteinaceous surface coat.

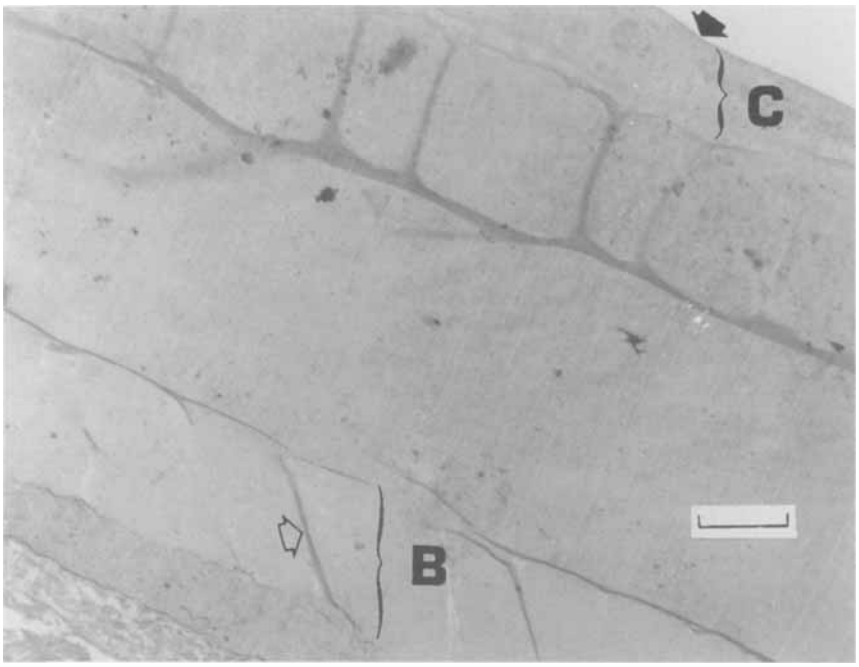


Figure 4. Transmission electron micrographs of *D. immitis* cuticle. Low magnification showing whole cuticle and the trilaminar membrane (closed arrow). Note close resemblance of median layer patterns (spanning between cortical and basal layers) to those in Figure 2. Also note basal striations (open arrow) (original magnification ×3300). Bar = 5 μm. (C) cortical layer, (B) basal layer, (G) glycocalyx. Both sections fixed in 4% glutaraldehyde followed by 2% osmium tetroxide and stained with uranyl acetate and lead citrate. Additional stains indicated in parenthesis.

Surface chemistry

As a result of both drying-induced surface roughness and the intrinsic surface chemistry of these specimens, contact angle data were found to be nonequilibrium values. With the exception of the low-surface-tension, cyclic saturated hydrocarbon called dicyclohexyl, each of the other test liquids utilized showed some penetration into the specimen surfaces after only brief contact times.

Nevertheless, adequate data were collected to allow calculation of these important surface energy terms (with the caution that thermodynamic equilibrium was not obtained):

Critical Surface Tension = 27.7 dynes/cm
Distributed Component = 26.2 dynes/cm
Particular Component = 22.2 dynes/cm

These terms are often reported as gamma C (Critical Surface Tension), gamma D (usually denoting the dispersive, van der Waals forces), and



Figure 5. High magnification of Figure 4 showing the glycocalyx external to the trilaminar membrane (closed arrow) (Ruthenium red stain, original magnification ×80,000). Bar = .1 μm.

gamma P (usually denoting the polar–polar interactions). The values obtained for the heartworm specimens are very similar to those previously measured and published for the intact vascular endothelium and for glutaraldehyde-preserved vascular grafts that show excellent long-term thromboresistance.

Figure 14 is an MAIR IR spectrum obtained with only a few, totally dried (in advance) heartworm segments clamped against it. This spectrum is almost identical to the clean prism baseline, and may be taken as the appropriate baseline for the remainder of the spectra provided here.

Figure 15 is the MAIR IR spectrum that resulted, after considerable experimentation, from the most successful method of securing intimate contact of the heartworm surfaces with the analytical prism. This method utilized specimens that were still completely hydrated after distilled water

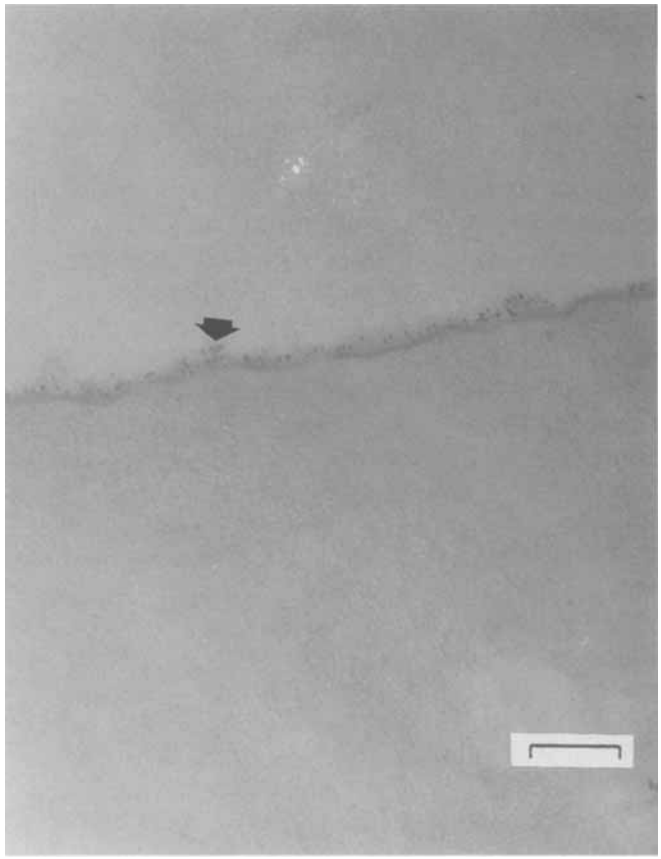


Figure 6. Transmission electron micrographs of ferritin-labeled cuticular surfaces (whole serum). Note even distribution of ferritin particles (closed arrow) (original magnification ×80,000). All specimens (Figs. 6–9) fixed in 4% glutaraldehyde followed by 2% osmium tetroxide and stained with uranyl acetate and lead citrate. Rabbit anti-dog antibodies used as primary layer. Specificity of primary antibodies listed separately for each. All bars = 0.1 μm.

rinsing away of the preservation solution. Figure 15 is, in fact, a typical spectrum for water as bound in a loose biological gel.

Figure 16 illustrates the conversion of this spectrum to that more characteristic of the actual heartworm surface as slow dehydration of the specimens was allowed to occur (adjusting the clamping pressure to maintain intimate specimen-to-prism contact throughout). Clearly, the emerging specimen signal is that of a predominantly glycoproteinaceous film.

Figure 17 is representative of the fully dehydrated specimen surfaces, a spectrum classically associated with glycoproteinaceous coatings.

Figure 18 is representative of the same specimens after even tighter clamping against the mini-Ge prism, to enhance spectral contrast.

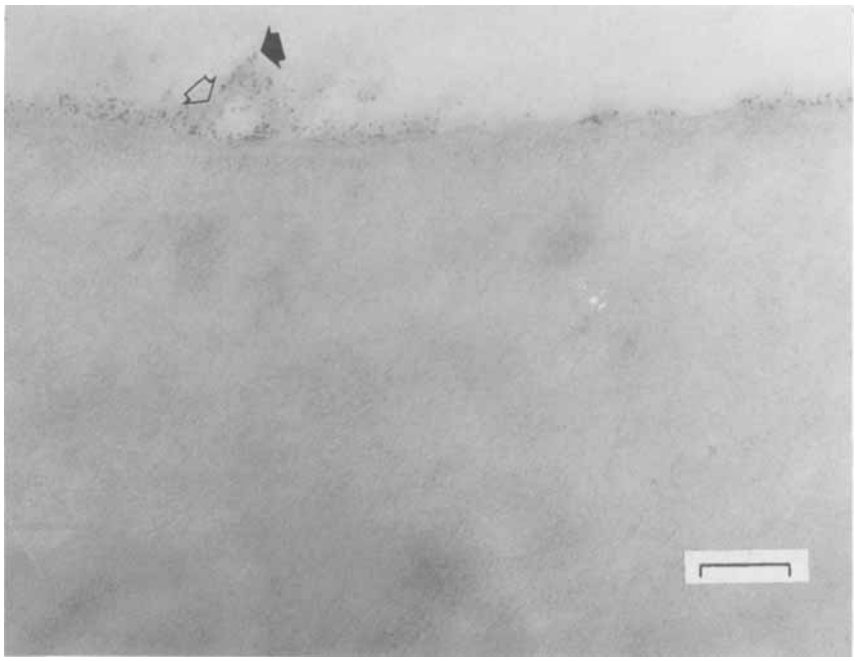


Figure 7. Albumin: Ferritin particles (closed arrow) formed a multi-layered coat over the thickness of the glycocalyx (open arrow) marking the abundance of adsorbed host albumin on surface (original magnification ×80,000). See Figure 6 for details.

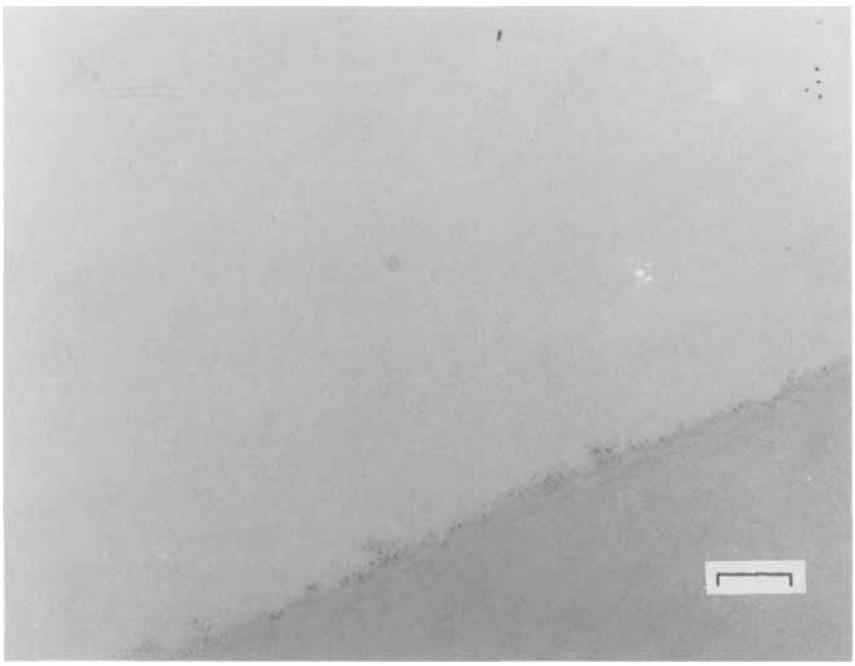


Figure 8. IgG (original magnification ×55,000). See Figure 6 for details.

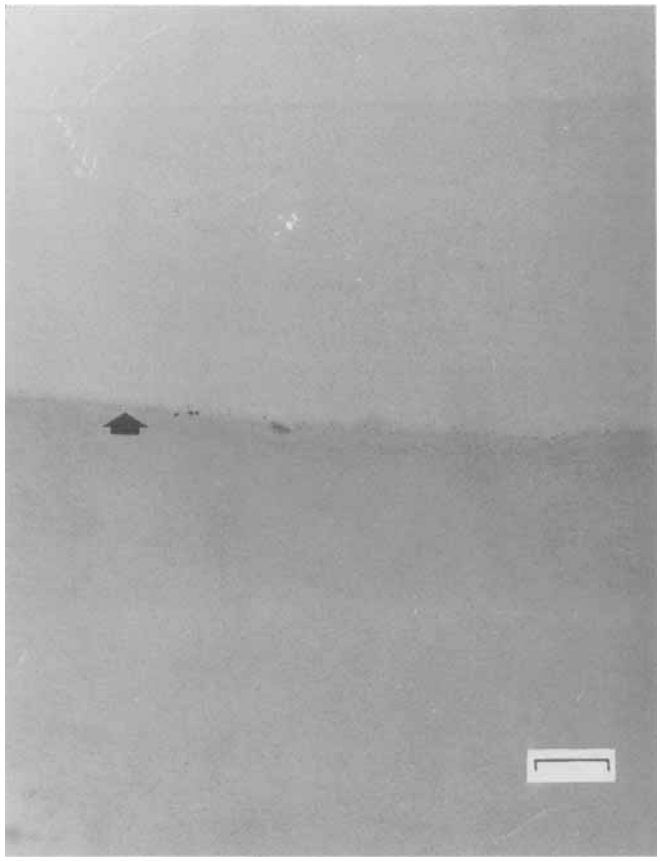


Figure 9. C3 (original magnification ×55,000). Note relatively low ferritin adsorption over the trilaminar membrane (closed arrow). See Figure 6 for details.

DISCUSSION

Lumsden[16] has already noted how "... the importance of surface phenomena in the biology of parasitic organisms is well appreciated ..." and that "... it is at the body surface that the host's defense mechanisms are often directed." The present study sought to elucidate the cuticular composition, morphology and surface reactivity (both physical–chemical and antigenic) of the adult *D. immitis*. The hypothesis is that a rational explanation of the mechanical, physiological, and immunological responses elicited by the parasite can emerge only from a good understanding of the morphology, surface chemistry, biochemistry, immunogenicity, and thrombogenicity of the external structures. In this respect, the cuticle and especially any adsorbed protein layers on the cuticular surfaces deserve special attention.

Although the morphology of the nematode cuticle, especially for *Ascaris*, *Trichnella*, and *Caenorhabditis* species has been extensively surveyed for both adult and larval stages, relatively little ultrastructural research has been con-

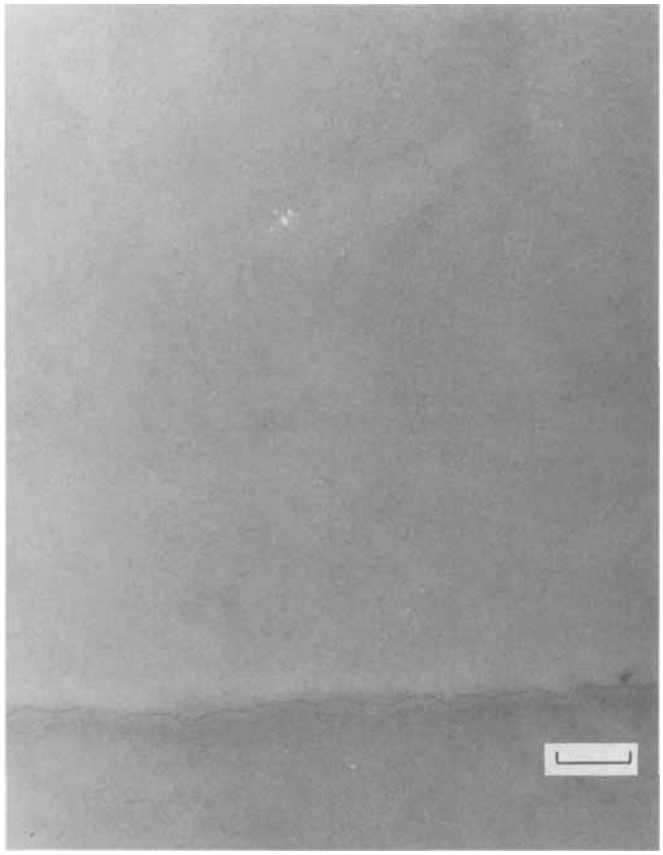


Figure 10. Transmission electron micrographs of primary antibody level control. Worms incubated in nonimmune rabbit whole serum followed by F-GAR-IgG. Nonspecific binding of primary antibody to surface antigens tested. All specimens (Figs. 10–13) fixed in 4% glutaraldehyde followed by 2% osmium tetroxide and stained with uranyl acetate and lead citrate. Note absence of ferritin adsorption to surfaces. All micrographs (Figs. 10–13) ×55,000. All bars = 0.1 μm.

ducted with the genus *Dirofilaria*, most of the available data consisting of SEM or light microscopy findings.[17,18] The present study shows that the cuticle of *D. immitis* fits into the classical description of a typical three layered nematode exoskeleton with basal, median and cortical layers, as proposed by Bird.[19]

The chemical composition of *Ascaris* cuticle has been studied by previous workers. Bird[19] characterized the proteins found in the cortical and median layers as keratin-like and collagen-like, respectively, unique to and characteristic of nematodes. Fujimoto and Kanaya[20] on the other hand, isolated another structural protein from the cuticle of the same parasite and coined

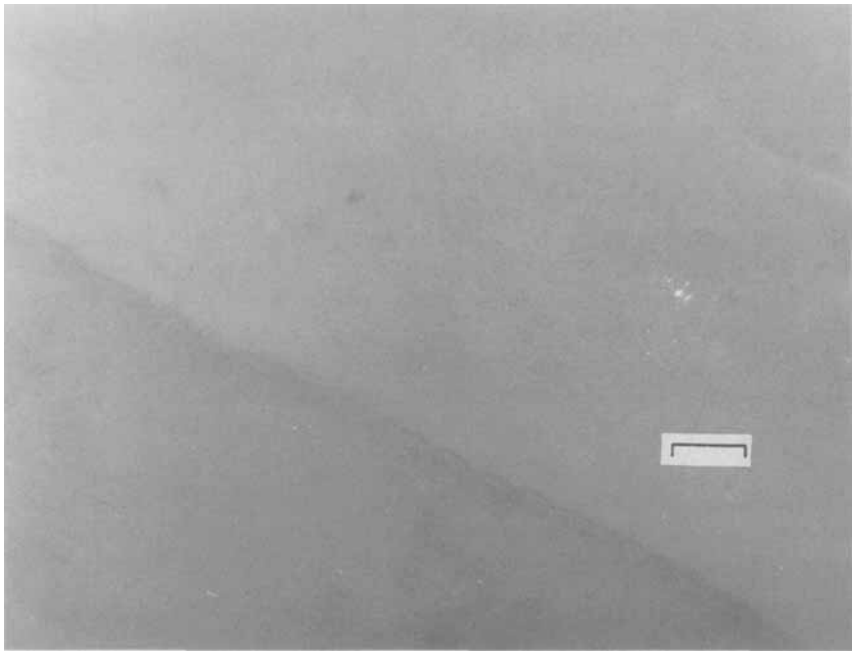


Figure 11. Secondary antibody control, I: Worms incubated directly in F-GAR-IgG, the primary antibody being omitted. Nonspecific binding between goat antibodies and dog antigens tested. See Figure 10 for details.

the term cuticulin for this new material. Although biochemical confirmation was not obtained in the present study, the histological observations do support the previous findings regarding nematode cuticular design and composition, in general. Collagen-like fibers (aniline blue-positive in histological and osmiophilic in TEM preparations) were observed to be wrapped around a keratin-like material (orange G positive and osmiophobic) in the median layer (Figs. 3, 4). These spirals probably correspond to the diagonal fibers crossing the *Ascaris* cuticle at an angle of about 75° to the longitudinal axis, as previously described.[21] It is known that collagen-like and keratin-like molecules give the cuticle its characteristic strength and stiffness, respectively. The particular arrangement for *D. immitis* detected in this study may provide the worm body with some extra degree of freedom in flexibility, still preserving the hardness and tensile strength required for survival.

An external glycocalyx and an internal trilaminar membrane were observed as the bounding surfaces of the cuticle. This new structural finding is potentially extremely important in understanding how several aspects of the host–parasite relationships are determined. Since the role of the trilaminar membranes in mediating ionic interactions and selective permeability is a well-known phenomenon for single mammalian cells, the interior cuticu-

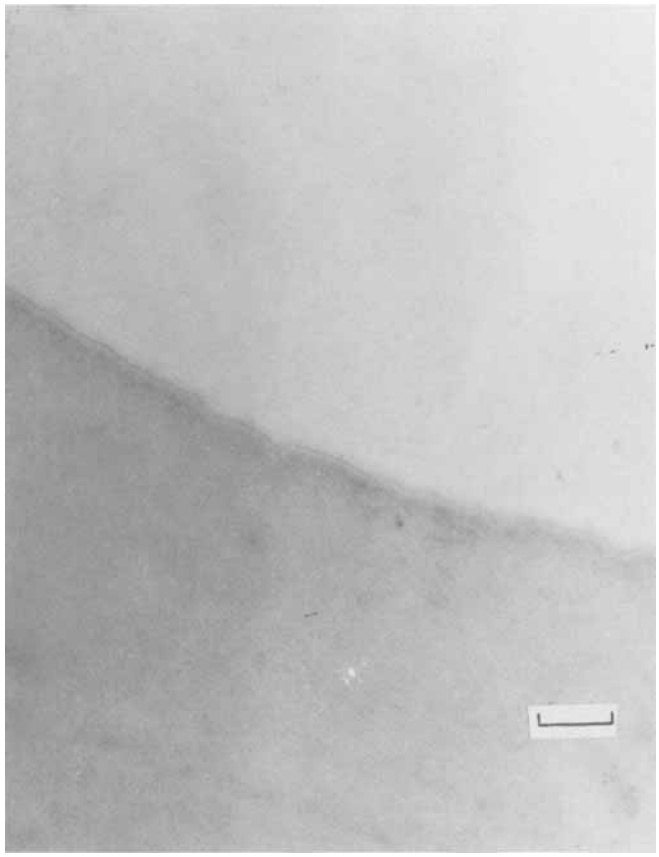


Figure 12. Secondary antibody control, II: Worms incubated in RAD-WS followed by unconjugated ferritin. Nonspecific binding of ferritin to primary antibody tested. See Figure 10 for details.

lar structure observed here may be speculated to perform similar functions. Another important feature of the trilaminar membrane could be that it provides attachment sites for negatively charged sugar molecules via integral proteins that contribute to its ultrastructure.[16] Such acidic mucopolysaccharides, apparently involved in attraction/repulsion interactions between parasite surfaces and host cells, have been proven to be present by experiments where destruction of surface charge with neuraminidase,[22] hyaluronidase and/or β-glucuronidase[16] facilitated attachment of leukocytes to cuticular surfaces and hence cuticular destruction, *in vitro*.[23] Although reticuloendothelial system cells have been observed on freshly recovered worm surfaces, it has been impossible to obtain evidence for *in vivo* destruction of the cuticle.

On the contrary, it is generally believed that animals infected with tissue helminths develop a suppressed cellular reaction while still being able to efficiently produce antibodies.[24] A possible explanation of the inhibition of

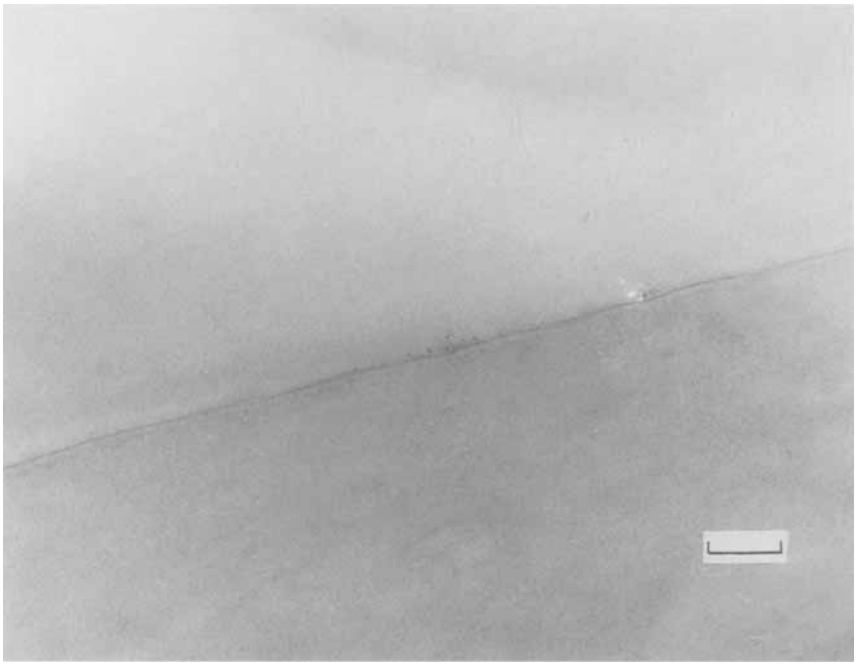


Figure 13. Surface level control: Surface proteins stripped off by soak in low pH, high ionic strength acetate-acetic acid buffer, prior to incubation in RAD-WS followed by F-GAR-IgG. Note adherence of few ferritin particles caused by insufficient stripping. See Figure 10 for details.

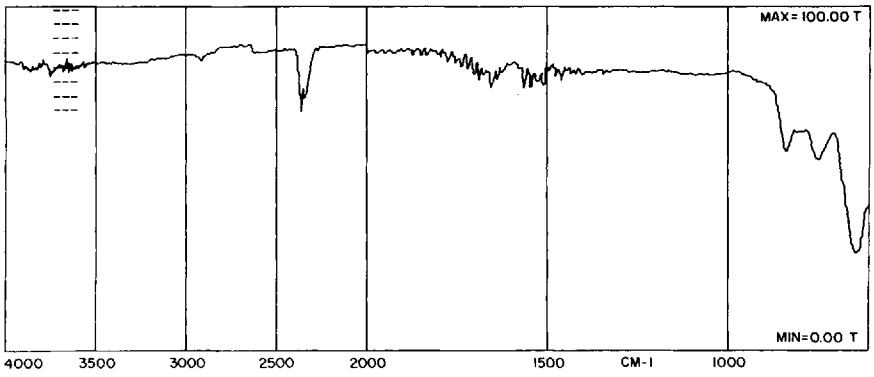


Figure 14. Baseline infrared spectrum.

the cellular component (including both phagocytic and sensitized cell populations) may be the very existence of the nonadhesive glycocalyx, providing the worm with an efficient barrier against cellular attachment and attack. Detection of anticuticular IgG on ferritin-labeled surfaces (Fig. 8), on the other hand, provides evidence of the persistent activity of the humoral

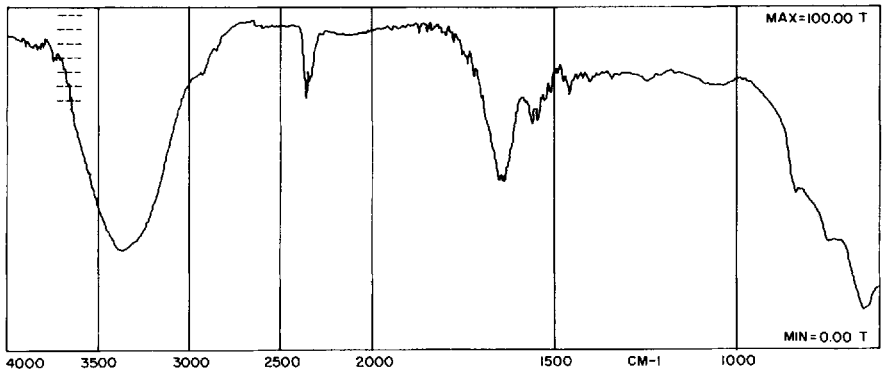


Figure 15. Infrared spectrum of fully hydrated cuticular surface of *D. immitis*.

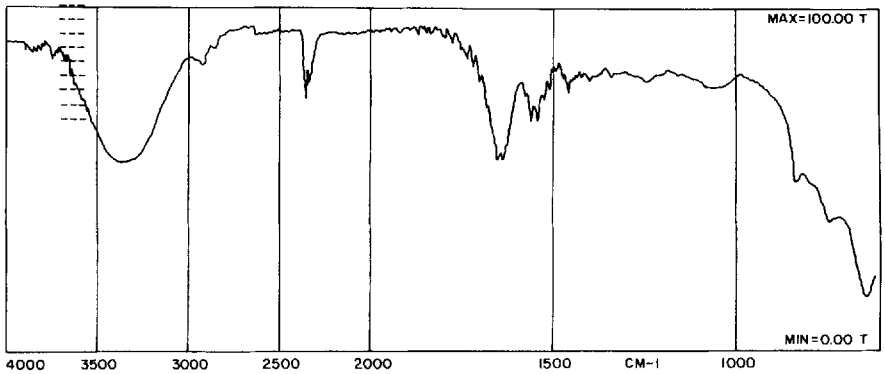


Figure 16. Improved spectrum of partially dehydrated surface zone of *D. immitis* cuticle.

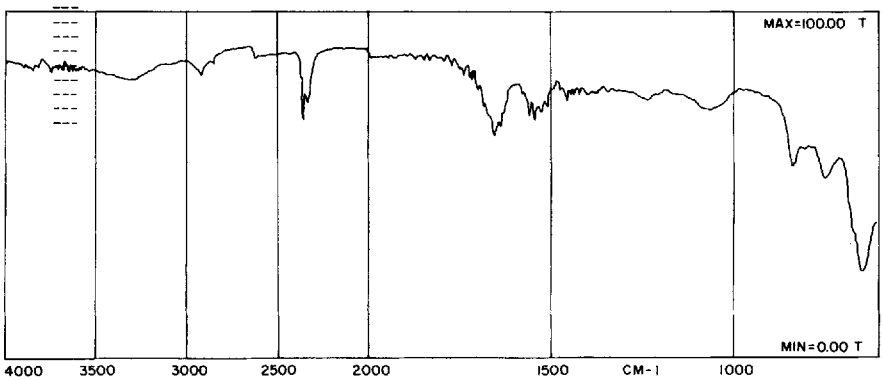


Figure 17. Infrared spectrum of fully dried *D. immitis* cuticular surface.

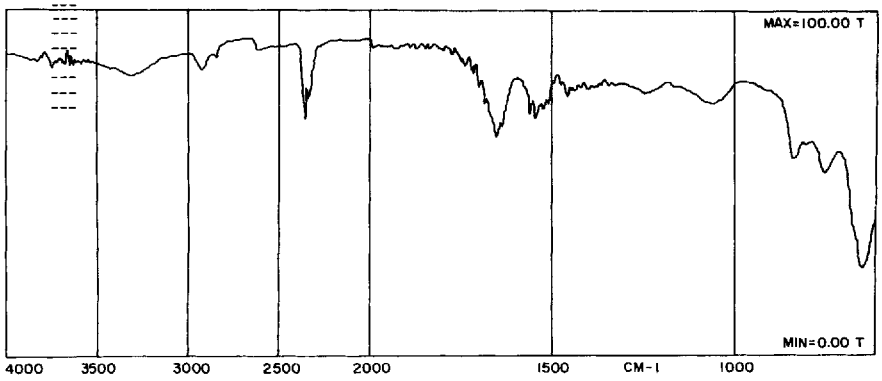


Figure 18. Confirming infrared spectrum of glycoproteinaceous matter dominating thromboresistant heartworm surfaces.

component. Although the amount of adsorbed protein was not quantified in this study, the continuous and sometimes multilayered distribution of ferritin made it obvious in RAD-IgG treated sections that quite a strong IgG reaction was elicited by the cuticle. Whether the bound IgG is *D. immitis* specific or it merely represents a cross-reacting result of sensitization to previous exposures to different parasitic immunogens can be determined with enzyme-linked immunosorbent assay (ELISA) as described earlier.[24]

The detection of host C3 on *D. immitis* surfaces (Fig. 9) also deserves particular attention. It is well known that parasite surfaces are potent activators of the alternative pathway of complement, a process that requires generation of enzymatically active C3b fraction by spontaneous hydrolysis of the highly reactive thioester bond incorporated in the free C3 molecule.[25] It may thus be understood how the incorporation of the available C3 on worm cuticular surfaces would result in blocking of the alternative pathway for activation via decreasing the plasma concentration of this C3b precursor. The operation of this mechanism would eventually lead to surface immunity to complement-dependent lysis.

Selective retention of host albumin (Fig. 7) on *D. immitis* cuticular surfaces may have a similar effect in transforming an essentially foreign and reaction-inducing surface into a host-like and inert one. Demonstration of bound albumin by the immunolabeling method described in this paper is in accord with previous data[11] and supports the view that adsorbed serum albumin from the host may serve the function of improved hemocompatibility, as proposed for foreign tissues and artificial surfaces,[26] by minimizing platelet retention and blood lysis.

The platelet retention studies provide strong support to this view, in that stripping of superficial protein layers was a significant factor in increasing platelet uptake.

Combining these findings with the infrared spectral data, the conclusion is inescapable that within the micrometer or so deep superficial layer, these heartworms are covered with a predominantly glycoproteinaceous sheath.

It is the outermost aspect of this proteinaceous superficial layer whose surface properties were characterized by the noted contact angle data. Overall, these data are very similar to results obtained on other bioadhesion-resistant surfaces, such as endothelial linings, intraoral mucosa, and the backs of dolphins and killer whales. Nature seems to solve the same problems in the same way in many, diverse circumstances.

This work was supported by the National Science Foundation Grant ECE-8504517, and the New York State Science and Technology Foundation. We thank Joan S. Hudson and Vonita A. Brown (Clemson University) for their help in specimen preparation for electron microscopy and histology, respectively.

References

1. R. E. Baier, "The basics of biomedical polymers: Interfacial factors," in *Polymeric Materials and Artificial Organs*, C. G. Gebelein (ed.), American Chemical Society, Washington, D.C., 1984, pp. 39–44.
2. G. D. Schmidt and L. S. Roberts, *Foundations of Parasitology*. 3rd Ed. The C. V. Mosby Co., St. Louis, 1985, p. 774.
3. A. F. Bird, "The nematode cuticle and its surface," in *Nematodes as Biological Models*, B. M. Zuckerman (ed.). Academic Press, New York, 1980, pp. 213–235.
4. P. V. Cherian, B. E. Stromberg, D. J. Weiner, and E. J. L. Soulsby, "Fine structure and cytochemical evidence for the presence of a polysaccharide surface coat of *D. immitis* microfilariae," *Int. J. Parasitol.*, **10,** 227–233 (1980).
5. Y. E. Spiegel, E. Cohn, and S. Spiegel, "Characterization of sialyl and galactosyl residues on the body wall of different parasitic nematodes," *J. Nematol.*, **14,** 33–39 (1982).
6. L. W. Bone and K. P. Bottjer, "Stimulation of feeding in *Trichostrongylus colubriformis* (Nematoda)," *Proceedings of the Helminthological Society of Washington*, **52,** 80–84 (1984).
7. R. Hordbring-Hertz and R. Mattiasson, "Action of a nematode-trapping fungus shows lectin-mediated host-microorganism interaction," *Nature*, **281,** 477–479 (1979).
8. L. W. Bone and K. P. Bottjer, "Cuticular carbohydrates of three nematode species and chemoreception by *Trichostrongylus colubriformis*," *J. Parasitol.*, **71,** 235–238 (1985).
9. J. B. Weiss, J. L. Magnani, and M. Strand, "Identification of *Schistosoma mansoni* glycolipids that share immunogenic carbohydrate epitopes with glycoproteins," *J. Immunol.*, **136,** 4275–4282 (1986).
10. A. P. Norden and M. Strand, "*Schistoma mansoni, S. haematobium,* and *S. japonicum:* Identification of genus-, species-, and gender-specific antigenic worm glycoproteins", *Exp. Parasitol.*, **57,** 110–123 (1984).
11. R. M. Maizels, M. Philipp, and B. M. Ogilvie, "Molecules on the surface of parasitic nematodes as probes of the immune response in infection," *Immun. Rev.*, **61,** 109–136 (1982).
12. C. R. Abramowsky, K. G. Powers, M. Aikawa, and G. Swinehart, "*Dirofilaria immitis,* 5. Immunopathology of filarial nephropathy in dogs," *Am. J. Pathol.*, **140**(1), 1–12 (1981).
13. N. P. Robertson and C. D. Cain, "Isolation and characterization of glycosaminoglycans from *Schistosoma mansoni*," *Comp. Biochem. Physiol.*, **82B**, 299–306 (1985).

14. B. Hammerberg, C. Dangler, and J. F. Williams, "*Teania taeniaeformis:* Chemical composition of parasite factors affecting coagulation and complement cascades," *J. Parasitol.*, **66**(4), 569–576 (1980).
15. C. M. McCormick, *A Platelet Retention Test Evaluation of Dirofilaria immitis*, M.S. Thesis, Clemson University, Clemson, SC, 1984.
16. R. D. Lumsden, "Surface ultrastructure and cytochemistry of parasitic helminths," *Exp. Parasitol.*, **37,** 267–339 (1975).
17. M. W. Wong and M. E. G. Brummer, "Cuticular morphology of five species of dirofilaria: A scanning electron microscope study," *J. Parasitol.*, **64,** 14 (1978).
18. C. M. Hendrix, M. J. Wagner, J. C. Schlotthauer, and B. E. Stromberg, "A scanning electron microscopic study of third-stage larvae of *Dirofilaria immitis*," *J. Parasitol.*, **70,** 149–151 (1984).
19. A. F. Bird, *The Structure of Nematodes.* Academic Press, New York, 1971, p. 318.
20. D. Fujimoto and S. Kanaya, "Cuticulin: A non-collagen structural protein from ascaris cuticle," *Arch. Biochem. Biophys.*, **157,** 1–6 (1973).
21. J. E. Harris and H. D. Crofton, "Structure and function of the nematodes: Internal pressure and cuticular structure in ascaris," *J. Exp. Biol.*, **34,** 116–130 (1957).
22. R. J. Hudson and W. D. Kitts, "Electrostatic forces affecting *in vitro* adherence of PMN leukocytes to the cuticle of protostrongylus larvae (nematoda)," *J. Parasitol.*, **57,** 808–814 (1971).
23. D. T. Morseth and E. J. L. Soulsby, "Fine structure of leukocytes adhering to the cuticle of *Ascaris suum* larvae II: PMN leukocytes," *J. Parasitol.*, **55,** 1025–1034 (1969).
24. G. J. Weil, E. A. Ottesen, and K. G. Powers, "*Dirofilaria immitis:* Parasite-specific humoral and cellular immune responses in experimentally infected dogs," *Exp. Parasitol.*, **51,** 80–86 (1981).
25. J. A. Bellanti, *Immunology—III,* Saunders, Philadelphia, 1985, p. 598.
26. D. J. Lyman, K. Knutson, B. McNeil, and K. Shibatani, "The effects of chemical structures and surface properties of synthetic polymers on the coagulation of blood—IV. The relation between polymer morphology and protein adsorption," *Trans. Am. Soc. Artif. Int. Organs,* **21,** 49–54 (1975).

Received October 13, 1988
Accepted February 17, 1989